Correlation of Stoichiometries for Rb + Extraction Determined by Mass Spectrometry and Electrochemistry at Liquid|Liquid Interfaces

ARTICLE *in* ANALYTICAL CHEMISTRY · JULY 2012

Impact Factor: 5.64 · DOI: 10.1021/ac301051e · Source: PubMed

3 AUTHORS, INCLUDING:

T. Jane Stockmann
Paris Diderot University
20 PUBLICATIONS **124** CITATIONS
SEE PROFILE

Zhifeng Ding
The University of Western Ontario
123 PUBLICATIONS **3,280** CITATIONS
SEE PROFILE

analytical chemistry

Article

pubs.acs.org/ac

Correlation of Stoichiometries for Rb^+ Extraction Determined by Mass Spectrometry and Electrochemistry at Liquid|Liquid Interfaces

Tom J. Stockmann, Anne-Marie Montgomery, and Zhifeng Ding*

Department of Chemistry, The University of Western Ontario, Chemistry Building, 1151 Richmond Street, London, Ontario, Canada N6A 5B7

Supporting Information

ABSTRACT: The electrochemical extraction of rubidium at micro water|1,2-dichloroethane (w|DCE) and water|room-temperature ionic liquid (w|RTIL) interfaces housed at the tip of a 25-μm capillary using octyl(phenyl)-*N*,*N*-diisobutylcarbamoylmethylphosphine oxide (CMPO) in the TRans Uranic EXtraction (TRUEX) process, was examined. Rubidium is of great interest in a modern spent nuclear fuel cycle as well as toward myocardial perfusion imaging utilizing $^{82}Sr/^{82}Rb$ isotopic generators. The ligand-to-metal stoichiometry (n:1) and overall complexation constant (β) for interfacial complexation reactions induced by an applied potential were determined by the interfacial electrochemistry. One stoichiometry, $n = 2$, was observed at the w|DCE interface with $\beta = 3.3 \times 10^4$. In the w|RTIL system, two rubidium salt solutions were employed: $RbNO_3$ and $RbNO_3$ plus Rb_2SO_4. The former demonstrated a stoichiometry of $n = 2$ and $\beta = 2.4 \times 10^6$, while the latter showed $n = 4$ and $\beta = 3.3 \times 10^{12}$. These stoichiometries of the reaction were confirmed by electrospray ionization mass spectrometry, using an emulsion generated by shaking water and DCE phases containing the dissolved metal and ligand, respectively. Both $RbCMPO^+$ and $RbCMPO_2^+$ complexes were observed. The influence of ion pair interactions in this system will be discussed.

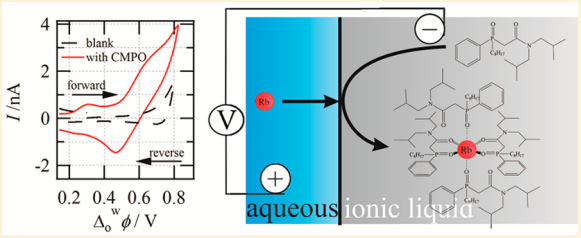

In 2002, Hoffert et al.[1] reviewed the contemporary perspectives on climate change, along with measures necessary to mitigate future adverse effects of anthropogenic CO_2 production from fossil fuels, particularly turning to alternative energy sources, including solar, wind, hydroelectric, fusion, and nuclear power generation. Barring the sudden implementation of an as-yet-unrealized technological advancement,[1,2] solar and nuclear power offer the only viable solution to the world's growing energy demands. While present concerns surrounding the exhaustion of fossil fuels have given rise to terms like "peak oil",[3] it is interesting to note that an analogous term could be applied to the present treatment of nuclear fuel (i.e., "peak uranium"). However, a parallel situation in the nuclear industry can be avoided, unlike the oil industry, through the use of breeder reactors and the implementation of a closed loop nuclear fuel cycle, whereby nuclear waste is recycled; such action could extend the life of the nuclear industry by hundreds of years.[1,4]

This strategy would also divert tonnes of radioactive material from entirely unnecessary proposed geological[5] and surface waste repositories, which are the subject of numerous controversies. Indeed, spent nuclear fuel (SNF) contains ~95% useable uranium,[6] with the other 5% coming from fission byproducts that are typically neutron absorbers, poisoning the fission reaction and reducing the efficiency of the fuel rod; should these impurities be removed, the efficiency would be restored. Similarly, these contaminants should be viewed as a potential resource; many of these isotopes have uses in medicinal[7−9] or other applications. This begs the question, however, as to the selectivity of current separation techniques and avenues of improvement.

Interestingly, alkali metals compose 6% of nuclear waste, including rubidium oxide;[6] however, little specific data seems to exist for the extraction of elements such as rubidium from SNF. Isotopes, such as ^{82}Rb, have been used in positron emission tomography for myocardial perfusion imaging and the diagnosis of coronary artery disease.[10−12] Strontium, which is another major component of SNF, has also found medicinal applications[7,13,14] and, therefore, distinguishing between Rb and Sr, along with their behavior in SNF reclamation streams, would be of special interest.

One contemporary separation method, called TRans Uranic EXtraction (TRUEX), uses the ligand octyl(phenyl)-*N*,*N*-diisobutylcarbamoylmethylphosphine oxide (CMPO) in a biphasic system composed of water and a paraffinic organic solvent, typically a *n*-dodecane/tributylphosphate mixture.[4,15] Presently, efforts to improve this process have been directed toward alternative solvents to replace *n*-dodecane; these include room-temperature ionic liquids (RTILs).[4,16−19] With the development of air stable versions and separate groups establishing the improved extraction efficiency obtained through their use,[16−19] RTILs have become a major focus in metal separation research.

Received: April 25, 2012
Accepted: June 17, 2012
Published: June 17, 2012

   dx.doi.org/10.1021/ac301051e | *Anal. Chem.* 2012, 84, 6143−6149

In a recent publication,[14] we showed that electrochemistry at a micro liquid|liquid interface between two immiscible electrolytic solutions (micro-ITIES)[20−22] can evaluate the interfacial complexation reactions easily and inexpensively. This specialized form of electrochemistry typically involves simple ion transfer (IT) and facilitated ion transfer (FIT) reactions, shown in eqs 1 and 2, respectively.

$$i_w^{z+} \rightleftharpoons i_o^{z+} \quad (1)$$

$$i_w^{z+} + nL_o \rightleftharpoons iL_{n,o}^{z+} \quad (2)$$

where metal species i, with charge $z+$, transfers from the aqueous phase, w, to the organic phase, o (or RTIL), through a push/pull mechanism controlled by an applied potential from an electrode immersed in each phase; here, the potential difference across the ITIES becomes the driving force, $\Delta_o^w\phi = \phi_w - \phi_o$. FIT is the electrochemical equivalent of ligand-assisted metal extraction. In the case of eq 2, the ligand, L, dissolved in the organic or RTIL phase improves the miscibility of i, typically a metal, which lowers the Gibbs energy of transfer and, in turn, the amount of applied potential necessary in order to elicit IT (see Figure S1 in the Supporting Information (SI)). Liquid|liquid electrochemistry has been the subject of numerous excellent reviews.[23−25]

Electrochemistry at an ITIES is commonly performed using water and 1,2-dichloroethane[22,26−29] (DCE) or nitrobenzene;[21] however, recent work in this field has expanded to include the w|RTIL interface.[14,30−35] Herein is described the FIT of rubidium using CMPO as a ligand dissolved in DCE and RTIL phases for the first time. Ion-pair phenomena has been explored through its effect on FIT at the w|RTIL interface by using two rubidium salts dissolved in the aqueous phase and comparing with only one salt. Additionally, the stoichiometry of interfacial complexation reactions was confirmed by electrospray ionization mass spectrometry, using an emulsion generated by two phase shaking.

EXPERIMENTAL SECTION

Chemicals. All purchased chemicals were of reagent grade and utilized without further purification, unless otherwise specified. 1,2-Dichloroethane (DCE), dichloromethane (DCM), trimethylchlorosilane, nitric acid, hydrochloric acid, rubidium sulfate (Rb_2SO_4), and rubidium nitrate ($RbNO_3$) were obtained from Fluka/Sigma−Aldrich (Sigma−Aldrich Canada, Ltd., Mississauga, ON). The RTIL component, trihexyltetradecylphosphonium chloride and CMPO were purchased from Strem Chemicals (Strem Chemicals, Inc., Newburyport, MA), while potassium tetrakis-(pentafluorophenyl)borate was ordered from Boulder Scientific (Boulder Scientific Company, Longmont, CO). Ultrapure Milli-Q water (18.2 MΩ) was used to generate all aqueous solutions. The preparation and characterization of our low-cost and very-hydrophobic RTIL, trihexlytetradecylphosphonium tetrakis(pentafluorophenyl)borate, were reported elsewhere.[35] The fabrication of micropipets[14,28,34,35] is outlined in the Supporting Information.

Electrochemistry. All electrochemical measurements were performed using the Modulab System from Solartron Analytical (Ametek Advanced Measurement Technology, Farnborough, Hampshire, U.K.). The Modulab is equipped with a femto ammeter, which was employed during all electrochemical experiments. A micropipet is incorporated into a modified HEKA pipet holder (HEKA Electronics, Mahone Bay, NS) and backfilled with the aqueous phase using a syringe. The pipet was then submerged into the RTIL or DCE phase in a glass vial held in a jacket mounted on a microstage, fabricated by our Electronic Shop in Chemistry at Western, and connected to a water circulator (VWR, Mississauga, ON) for heating. The RTIL and DCE experiments were conducted at 60 °C and room temperature, respectively. The following electrochemical cells were used:

$$\mathrm{Ag}\,|\,\mathrm{AgNO_3}\,|\,\underset{(aq)}{\text{5 mM } \mathrm{RbNO_3}}\,\|\,\underset{(DCE)}{\begin{matrix}\text{y mM CMPO}\\ \text{5 mM } \mathrm{P_{66614}TB}\end{matrix}}\,|\,\mathrm{AgTB}\,|\,\mathrm{Ag} \qquad \text{Cell 1}$$

$$\mathrm{Ag}\,|\,\mathrm{AgNO_3}\,|\,\underset{(aq)}{\text{5 mM } \mathrm{RbNO_3}}\,\|\,\underset{(\mathrm{P_{66614}TB})}{\text{y mM CMPO}}\,|\,\mathrm{AgTB}\,|\,\mathrm{Ag} \qquad \text{Cell 2}$$

$$\mathrm{Ag}\,|\,\mathrm{AgNO_3}\,|\,\underset{(aq)}{\begin{matrix}\text{2 mM } \mathrm{Rb_2SO_4}\\ \text{2 mM } \mathrm{RbNO_3}\end{matrix}}\,\|\,\underset{(\mathrm{P_{66614}TB})}{\text{y mM CMPO}}\,|\,\mathrm{AgTB}\,|\,\mathrm{Ag} \qquad \text{Cell 3}$$

In order to ensure that the interface remained at the tip of the micropipet, the micro-ITIES was monitored continuously through the use of a USB CCD camera (Motic, Richmond, BC) attached to a variable 12× magnifying lens assembly (Navitar, Rochester, NY).[14] Because of the low current employed in these electrochemical experiments, a two-electrode system was used. The working electrode (WE) lead of the potentiostat was attached, using a BNC connector to the pipet holder which, in turn, contains an integrated silver wire immersed in the aqueous phase. The counter electrode (CE) and reference electrode (RE) leads were connected to a silver wire placed in the DCE or RTIL phase.

Electrospray Ionization Time-of-Flight Mass Spectrometry (ESI-TOF MS). A Micromass LCT Mass Spectrometer (Waters, Milford, MA, USA), operating in the positive-ion mode, with capillary, sample cone, and extraction cone voltages of 5000, 25, and 0 V, respectively, were used for all electrospray ionization time-of-flight mass spectrometry (ESI-TOF MS) measurements. The sample time, scan time, and interscan delay were set to 5 min, 4 s, and 0.1 s respectively. An emulsion was generated by shaking water and DCE phases containing the dissolved metal and ligand, respectively. The emulsion of interest was loaded into a 250-μm syringe (Hamilton Co., Reno, NV, USA) and placed in a syringe pump (Hamilton Co.) operating at 25 μL min^{-1}. Isotopic distribution modeling was carried out using the "Molecular Weight Calculator", which is a Freeware program developed by Matthew Monroe at Pacific Northwest National Laboratory and available via the Internet.[36]

RESULTS AND DISCUSSION

Facilitated Ion Transfer Rb^+ at the w|DCE Micro-ITIES Using CMPO. Figure 1A shows a typical cyclic voltammogram (CV) acquired using Cell 1 with no CMPO present in the DCE phase (y = 0). The CV was initiated at a Galvani potential difference of 0.127 V and scanned in the forward direction toward more positive potentials until 0.525 V was reached. Here, an increase in current can be observed that is indicative of the transfer of the supporting electrolytes (Rb^+ from water to

dx.doi.org/10.1021/ac301051e | Anal. Chem. 2012, 84, 6143−6149

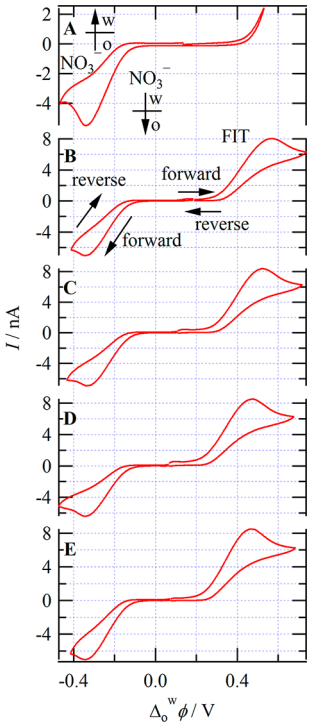

Figure 1. Cyclic voltammograms (CVs) acquired using Cell 1 with (A) $y = 0$, (B) $y = 14$ mM of CMPO, (C) $y = 39$ mM of CMPO, (D) $y = 60$ mM of CMPO, and (E) $y = 78$ mM of CMPO. Two regions were swept independently, with the following parameters: a scan rate of 0.020 V s^{-1}, an initial potential of 0.070 V, and upper and lower limits of 0.675 and −0.450 V, respectively.

organics and TB^- from organics to water); this sharp increase in current describes the limit of the polarizable potential window (PPW). From here, the potential was swept in the reverse direction to −0.492 V. During the reverse scan, a peak shaped wave was observed with a peak potential of −0.342 V; this is attributed to the IT of nitrate anions from water to organics.

The half-wave potential of NO_3^- IT was used as an internal reference for the purposes of calibrating the potential scale through the use of the TATB or Parker's assumption;[37−39] the formal transfer potential, $\Delta_o^w\phi^{o\prime}_{tr,NO_3^-}$, at the wlDCE ITIES was taken to be −0.314 V.[40] The half-wave potential of NO_3^- IT was determined using its peak potential and eq 3 from Bard and Faulkner.[41]

$$E_{1/2} = E_p \pm \frac{0.028\ \text{V}}{z_i} \tag{3}$$

The potential was then swept in the positive direction from −0.492 V to 0.127 V, where a sigmoidal shaped wave with a steady-state current was observed that is indicative of simple NO_3^- IT back across the ITIES from organics to water.

This asymmetrical current response is typical of IT at a micro-ITIES housed at the tip of a micropipet and agrees well with established theory.[26,27] This asymmetry is a direct result of the physical geometry of the pipettes. Please note that if the CV range is increased at the positive end, an exponential increase in the current response is observed and may result in a disruption of the interface; an example is shown in Figure S2 in the Supporting Information.

The potential scale was calibrated through the TATB assumption[37−39] via the following equation:

$$\Delta_o^w\phi^{o\prime}_{ML_n^{z+}} - \Delta_o^w\phi_{1/2,ML_n^{z+}} = \Delta_o^w\phi^{o\prime}_{NO_3^-} - \Delta_o^w\phi_{1/2,NO_3^-} \tag{4}$$

Please note that all CV results have undergone this treatment using nitrate as an internal standard.

Figure 1 illustrates CVs obtained as the concentration of CMPO on the DCE phase is increased; Figures 1B, 1C, 1D, and 1E show the system with 14, 39, 60, and 78 mM of CMPO, respectively. Each CV was scanned in two parts using a scan rate of 0.020 V s^{-1}.

At first the system was scanned in the negative direction from ∼0.070 V to −0.450 V, returning to 0.070 V; this segment, again, details NO_3^- IT.

The second section was from an initial potential of ∼0.070 V to 0.670 V and back; during this sweep, a peak current can be observed during the forward scan with peak potentials of 0.567, 0.511, 0.470, and 0.469 V for the respective curves in Figures 1B, 1C, 1D, and 1E. This peak-shaped wave is indicative of the FIT of Rb^+ from water to organics via a mechanism referred to as transfer by interfacial complexation (TIC) with the CMPO ligand.[42] The reverse sweep shows a sigmoidal-shaped current response, and this is indicative of transfer through interfacial decomplexation (TID).[42]

Interestingly, as the concentration of the ligand in the DCE phase increases, the FIT peak shifts to more-negative potentials. This trend, along with both current response features are in good agreement with the theory of FIT at a micro-ITIES held at the tip of a micropipet, as established by the pioneering work of Homolka et al.,[21] Kakiuchi and Senda,[20] and Girault et al.[22,42,43] and demonstrated recently.[14,28]

Figure 2A shows a linear relationship developed over a series of CMPO concentrations by graphing $zF/(RT)$ $(\Delta_o^w\phi^{o\prime}_{ML_n^{z+}} -$

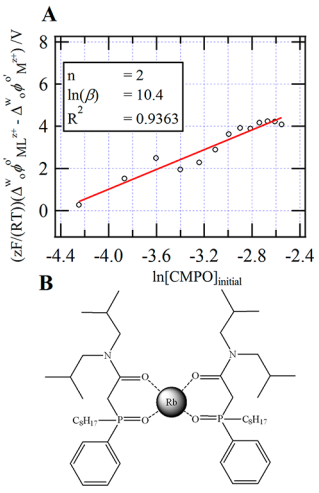

Figure 2. (A) Plot of $zF/(RT)(\Delta_o^w\phi^{o\prime}_{ML_n^{z+}} - \Delta_o^w\phi^{o\prime}_{M^{z+}})$ versus $\ln[\text{CMPO}]_{\text{initial}}$. (B) Proposed structure for $RbCMPO_2^+$.

$\Delta_o^w\phi^{o\prime}_{M^{z+}})$ versus $\ln[\text{CMPO}]_{\text{initial}}$. As developed by Girault et al.,[22] the linear relationship can be used to determine the stoichiometry (n) and overall complexation constant (β) (see eq 5):

$$\frac{zF}{RT}(\Delta_o^w\phi^{o\prime}_{ML_n^{z+}} - \Delta_o^w\phi^{o\prime}_{M^{z+}}) = n\ln(c_{init}) + \ln(\beta) + \ln(\xi) \tag{5}$$

where z, F, R, and T are the conventional thermodynamic constants of charge, Faraday's constant, the universal gas

dx.doi.org/10.1021/ac301051e | Anal. Chem. 2012, 84, 6143−6149

constant, and temperature (in Kelvin); $\Delta_o^w\phi_{ML_n^{z+}}^{o\prime}$ is the formal transfer potential of the metal−ligand complex obtained from the CV; $\Delta_o^w\phi_{M^{z+}}^{o\prime}$ is the free metal formal transfer potential equal to 0.576 V, which was estimated through simple IT at a micro-ITIES;[44,45] and $\xi = (D_O/D_W)^{1/2}$, such that D_W and D_O are the diffusion coefficients in the aqueous and organic phases. It is assumed that the diffusion of species in either phase is equivalent so that the final term is removed and eq 5 is greatly simplified.

The half-wave potentials for FIT were determined using eq 3 and calibrated with eq 4, through the TATB assumption.[37−39]

The linear relationship is such that the slope is the ratio of ligand to metal (n:1), and the intercept is the natural logarithm of the overall complexation constant. Using regression analysis, a linear curve fitting was applied to the data, giving a slope of 2 and a y-intercept of 10.4 ± 0.6 with R^2 = 0.9363. Therefore, because of the reasonable linear fit, it can be concluded that a stoichiometry of 2 CMPOs for each metal, as illustrated by Figure 2B with an overall complexation constant of 3.3×10^4, was obtained.

Many alkali-metal complexes[46−51] have been reported and alkali coordination chemistry is frequently reviewed.[52] Dissolved in water, a rubidium ion typically has an inner hydration sphere consisting of 8 coordinate water molecules[53] and this relatively high coordination number (cn) is also reflected in its ligand/complexation chemistry with typical cn range of 6−8.[46−51] Recently, Chekhlov[50] elucidated the crystal structure of (2,2,2-cryptand)rubidium chloride and bromide such that the six oxygens and two nitrogens on cryptand were coordinated to the metal center. Interestingly, Meng[54] reported the crystal structure of poly[(μ-2-hydroxy-3,5-dinitrobenzoato)rubidium] in which the rubidium center is coordinated to 10 oxygens from eight 3,5-dinitrosalicylate complexes with $\pi-\pi$ stacking between these groups contributing to the stability of the compound. This is further evidence toward the viability of the ligand stoichiometry determined voltammetrically for Rb with CMPO, indicating that steric hindrance is not a issue in this case.

In fact, the coordination of 2−3 CMPOs to a metal center seems typical[14,17,55,56] and a proposed $RbCMPO_2^+$ structure is shown in Figure 2B.

Interfacial Complexation Stoichiometry Determined by Mass Spectrometry. In order to confirm the ligand to metal stoichiometry (n:1) observed at the w|DCE interface, direct injection of an emulsified aqueous/DCE solution generated through a shake flask experiment, into an ESI-MS was performed.[14] One hundred microliters (100 μL) of a 20 mM $RbNO_3$ aqueous solution and 100 μL of 100 mM CMPO in DCE were placed in a small flask, where they were mixed by shaking. The formed emulsion was subsequently injected into the ESI-MS analyzer. Figure 3 depicts a typical mass spectrum highlighting the experimental region, corresponding to $[RbCMPO]^+$ and $[Rb(CMPO)_2]^+$. The insets in the figure illustrate the calculated (red, or top inset) and experimental (blue, or bottom inset) isotopic distribution profiles at 493.2 and 900.4 Th, respectively. There are two naturally occurring isotopes of Rb: ^{85}Rb and ^{87}Rb, with abundances of ∼72.17% and ∼27.83%, respectively.[57] Interestingly, these isotopes are reflected in the calculated profile for $[RbCMPO]^+$ with two large peaks separated by 2 Th; the other peaks, at intervals of 1 Th, are typical of hydrocarbon material with a charge of 1+.

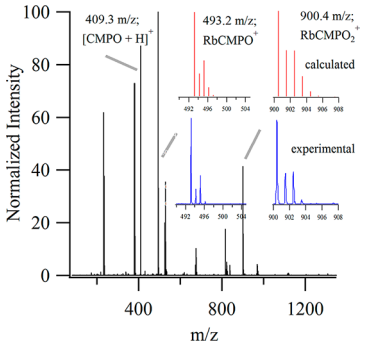

Figure 3. Mass spectrum of the emulsion formed with 100 μL of 20 mM $RbNO_3$ aqueous solution and 100 mM CMPO in DCE. Inset: the isotopic distribution of $RbCMPO^+$ and $RbCMPO_2^+$ calculated (red, or top insets) and experimental (blue, or bottom insets).

The $RbCMPO_2^+$ complex observed spectroscopically corroborates the electrochemical data. The investigation of alkali-metal complexes using ESI-MS was also demonstrated by Leize et al.[46] and Lawerance et al.[49] In both articles, the authors reported avoiding a biphasic system by using either a methanol:water mixture[46] in order to dissolve the ligands and metals in one solution, or through the use of short-chain alcohols as ligands,[49] which could be dissolved easily in water. Leize et al.[46] used 18-crown-6 ether (18Cr6) and cryptand-[2,2,2] as ligands and observed 1:1 metal-to-ligand complexes for Li, Na, and K but for Rb and Cs, with 18Cr6, they also observed sandwich compounds of 1:2 ratios. This earlier discovery using 18Cr6 also serves to demonstrate that higher cn in Rb complexes are possible; giving a total cn of 12. These findings, presented herein, correlate well with the literature.

It is interesting to note that, while the potential difference across this emulsified interface was not measured, the shaking process resembled a simple open circuit potential experiment and assisted rubidium ion transfer along with the CMPO ligand from water to organics.

Facilitated Ion Transfer of Rb^+ at the Micro w|RTIL interface Using CMPO. Figure 4 shows typical CVs acquired at an w|RTIL micro-ITIES using Cell 2 for curves A, B, C, and D with CMPO concentrations (y) equal to 0, 30, 44, and 69 mM while curves E, F, G, and H used Cell 3 and y values of 0, 60, 70, and 90 mM, respectively.

Trace A in Figure 4 illustrates the current response versus the applied Galvani potential difference with no CMPO added to the RTIL phase (i.e., a blank solution). The potential was swept linearly starting at 0.184 V and progressing toward more positive potentials with a scan rate of 0.010 V s^{-1}. The edge of the PPW was reached at ∼0.782 V, which was limited by the transfer of the supporting electrolytes: Rb^+ from water to RTIL and the anionic component of the RTIL (TB^-) from RTIL to water. The CV was subsequently swept in the reverse direction, toward more negative potentials form 0.782 to −0.365 V; a peak-shaped wave was observed at −0.333 V, and this is attributed to the simple IT of NO_3^- from water to the RTIL. The edge of the PPW, at the negative end, is limited by the transfer of the cationic component of the RTIL (P_{66614}^+). The potential was then scanned in the forward direction, with a final potential of ∼0.184 V. A second peak-shaped wave was observed during this final segment with a peak potential at −0.078 V; this is attributed to the IT of nitrate back across the ITIES. Unlike at the w|DCE interface, the w|RTIL experiences diffusion control in both directions, whereby ion transfer from

dx.doi.org/10.1021/ac301051e | Anal. Chem. 2012, 84, 6143−6149

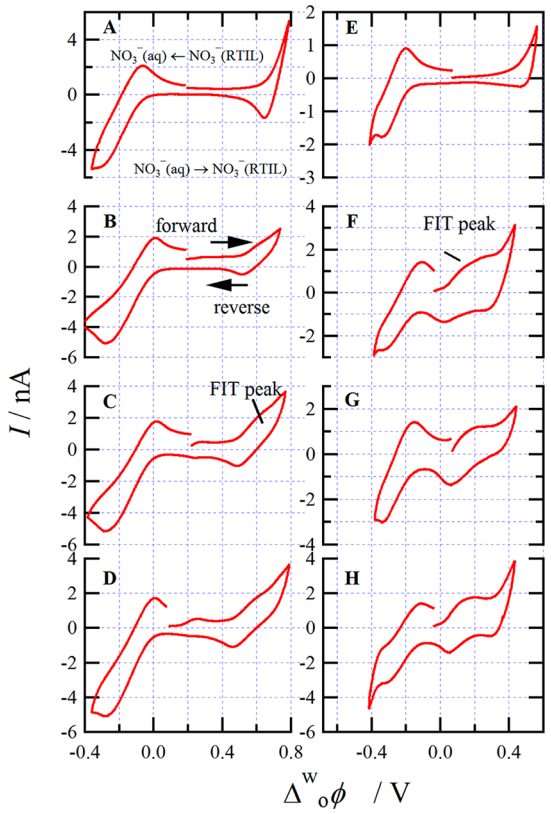

Figure 4. Plots of cyclic voltammograms (CVs). Curves A, B, C, and D were taken using Cell 2 with y = 0, 30, 44, and 69 mM, respectively, and a scan rate of 0.010 V s^{-1}. Curves E, F, G, and H were acquired using Cell 3 with y = 0, 60, 70, and 90 mM, respectively, and all of these CVs used a scan rate of 0.020 V s^{-1}.

outside to inside the pipet is affected by the high viscosity of the RTIL phase (i.e., low diffusion coefficient). These observations of IT at an w|RTIL interface are in good agreement with the pioneering works of Kakiuchi et al.[30,31,58] and Samec et al.,[32,33] as well as our recent publications.[14,35]

Interestingly, with the addition of CMPO to the RTIL phase, another peak can be observed in the forward and reverse scans; similar to the w|DCE case, this is attributed to the FIT of Rb^+ through TIC during the forward sweep and TID when the potential is scanned back. This peak shifts from 0.595, 0.587, and 0.580 V for curves B, C, and D using Cell 2, which contains only $RbNO_3$ in the aqueous phase and y = 30, 44, and 69 mM CMPO in the RTIL phase, respectively. The half-wave potentials for FIT and IT were taken to be the midpoint between their respective forward and reverse transfer waves, which were then treated using eq 4 in order to determine the formal transfer potential of the metal−ligand complex.

A similar relationship to w|DCE can be developed at the w| RTIL ITIES for FIT; however, the final term in eq 2, $\ln(\xi)$, as well as the free-metal transfer potential of Rb, $\Delta^w_{RTIL}\phi^{o\prime}_{Rb^+}$, must be evaluated to obtain the complexation equilibrium constant.

$\Delta^w_{RTIL}\phi^{o\prime}_{Rb^+}$ was taken to be 0.706 V and was obtained through a working curve for the microinterface by means of Comsol Multiphysics software, through finite-element analysis, similar to the numerical approach in the case of a large interface by Girault et al.[44] This working curve method utilizes the ratio between the current at the edge of scan, I_{eos}, and the return peak current, I_{rp}, (I_{eos}/I_{rp}), developing a relationship with this normalized current and the return peak potential, E_{rp}. This technique for finding the formal transfer potential of species limiting the PPW was first demonstrated by Girault et al.[44] at a large (centimeter scale) w|DCE ITIES, where a well-defined return peak is observed.

ξ was estimated using the diffusion coefficient of ferrocene in $P_{66614}TB$, D_w^{FC} = 3.5 × 10^{-8} cm^2 s^{-1}, to represent the ligand/complex, while the diffusion coefficient of tetramethylammonium (TMA^+), $D_w^{TMA^+}$ = 2.0 × 10^{-5} cm^2s^{-1}, was used for the free metal in the aqueous phase.[35] Ferrocene is a relatively large organometallic compound; thus, it is a good approximation toward the metal−ligand complex and its movement through the RTIL medium. The van der Waals radius for rubidium is listed as 3.03 Å,[59] which is comparable to the size of TMA^+,[60,61] and while this does not take into account specific intermolecular forces, it is believed to establish a good analogue for metal diffusion through an aqueous solution. In addition, while Rb^+ transfer cannot be observed within the PPW, TMA^+ can; therefore, its diffusion coefficient can be readily determined through facile CV experiments.

It is important to note that these approximations will only have an effect on the determination of the overall complexation constant and do not influence the evaluation of the metal−ligand stoichiometry.

Based on these assumptions, the linear relationship between $[zF/(RT)](\Delta^w_o\phi^{o\prime}_{ML_n^{z+}} - \Delta^w_o\phi^{o\prime}_{M^{z+}})$ and $\ln[CMPO]_{initial}$ for Cell 2 was developed and is shown in Figure 5; the overall

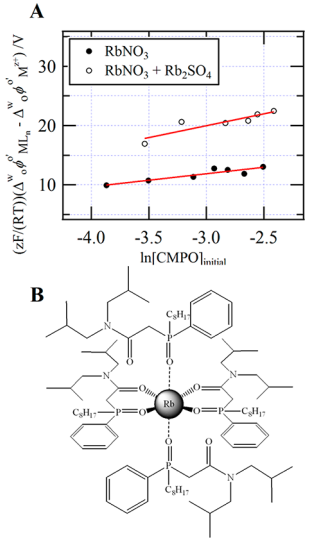

Figure 5. (A) Plot of $[zF/(RT)](\Delta^w_o\phi^{o\prime}_{ML_n^{z+}} - \Delta^w_o\phi^{o\prime}_{M^{z+}})$ versus $\ln[CMPO]_{initial}$ with metal−ligand transfer potentials obtained from CVs shown in Figure 4. (B) Proposed structure of $RbCMPO_4^+$.

stoichiometry for Cell 2 was determined to be 2, with ln β = 18.4 ± 1.3 or a complexation constant of 2.4 × 10^6 with an R^2 value of 0.9165, demonstrating reasonably good linear correlation.

Interestingly, the stoichiometry from Cell 2 closely mirrors that obtained at the w|DCE interface for Cell 1; however, the complexation constant is 73 times higher. Using conventional means of extraction, the distribution ratio of the metal species has been shown to be higher in water−RTIL separations versus traditional molecular organic solvents;[16,18,19] therefore, the present result is in good agreement with these previous reports, because it further illustrates the improved extraction capabilities

dx.doi.org/10.1021/ac301051e | Anal. Chem. 2012, 84, 6143−6149

of RTILs versus organic solvents, as was also demonstrated by our group recently.[14]

In the case of Cell 2, the peak-to-peak separations for the forward and reverse FIT and simple IT are high, with average values of 150 and 280 V. It was proposed that this may be due to a lack of electrolytes in the aqueous phase, since $RbNO_3$ was both an analyte and a supporting electrolyte; since Rb^+ and NO_3^- ions are transferred, a depletion zone may be generated near the ITIES, so that no charge carriers are present, resulting in a resistance increase and an increase in peak-to-peak separation. In order to test this, Cell 3 was employed; only rubidium salts were used, to avoid unwanted complexation with alternative metal salts, which may lead to ambiguous results.

Similarly, for Cell 3, containing both 2 mM $RbNO_3$ and 2 mM Rb_2SO_4 in the aqueous phase, the FIT peak shifts from 0.230 to 0.178 and 0.140 V is shown in Figures 4E, 4F, 4G, and 4H with CMPO concentrations of 0, 60, 70, and 90 mM, respectively, using a scan rate of 0.020 V s^{-1}. In the same way as Cell 2, the stoichiometry and complexation constant for Cell 3 were determined to be 4 and 3.3×10^{12} ($\ln \beta = 31.982 \pm 0.3$), respectively, with the linear curve fitting shown in Figure 5A; and an R^2 value of 0.8992 shows a satisfactory linear trend. Figure 5B shows the proposed structure of $RbCMPO_4^+$ with two CMPOs coordinating in a bidentate fashion and the remaining two through a single phosphine oxide, giving an overall octahedral geometry.

Interestingly, using the Rb_2SO_4 salt in conjunction with $RbNO_3$ reduced the peak-to-peak separation to 0.065 and 0.250 V for FIT and IT, respectively. However, the stoichiometry changed from 2 to 4, which may be due to increased ion-pair formation or coordination between Rb^+ and SO_4^{2-}. Analogous to the metal electrode, the liquid|liquid interface has been described using a Gouy−Chapman model[62] as a compact interface with two back-to-back diffuse layers where non-Faradaic processes, such as the absorption of a chemical species, can occur. Thus, Rb^+ and NO_3^- ions may aggregate at the ITIES and interact or associate more closely, allowing for intermolecular interactions and ion pair formation. These interactions may be strong enough to influence IT or FIT, thus leading to a change in stoichiometry. Recently, Girault et al.[45] demonstrated that metal salts paired with different anions could suffer a change in the free-metal ion transfer potential at an w|DCE microhole ITIES. An analogous phenomena may also be at work here, increasing the number of CMPO molecules necessary to induce FIT.

$RbCMPO_4^+$ was not observed using ESI-MS, despite injecting an emulsion generated by shaking the water phase containing 2 mM $RbNO_3$ and 2 mM Rb_2SO_4 with a DCE phase containing 100 mM CMPO (data not shown); however, the other stoichiometries of 1 and 2 were still present. In a recent publication,[14] we showed, for the analysis of strontium complexation with CMPO, this simple "shake" flask experiment was comparable to the more-sophisticated biphasic electrospray ionization mass spectroscopy (BESI-MS) technique, and confirmed the stoichiometry observed voltammetrically: $SrCMPO_2^{2+}$ and $SrCMPO_3^{2+}$. A BESI-MS/MS dispersion study[14] showed that the third CMPO was easily lost, producing a marked increase in the $SrCMPO_2^{2+}$ ion peak.[14]

A similar phenomenon may be occurring with Rb and CMPO, whereby the two additional CMPOs determined in $RbCMPO_4^+$ are only weakly associated and cannot be observed through ESI-MS. The ESI-MS data are in good agreement with the stoichiometry obtained electrochemically. The direct injection of an aqueous/RTIL emulsion was deemed unadvisible; first, the viscosity of the RTIL is prohibitive against its direct injection, and, second, the ionic components would most likely mask any signal from the RbCMPO complex, because of their high signal.

CONCLUSIONS

The FIT of the rubidium ion at micro liquid|liquid interfaces was reported. At the w|DCE interface, a ligand to metal stoichiometry of 2:1 and a complexation constant of 3.3×10^4 were determined. At the w|RTIL micro-ITIES, two rubidium salts ($RbNO_3$ and Rb_2SO_4) were employed. First, only $RbNO_3$ was dissolved in the aqueous phase and the ligand-to-metal ratio was found to be 2:1, with an overall complexation constant of 2.4×10^6, which is 73 times higher than that obtained at w|DCE. An aqueous solution of $RbNO_3$ with Rb_2SO_4 was used to help improve the level of supporting electrolyte, which decreased the peak-to-peak separation of the FIT forward and reverse waves and resulted in a ligand-to-metal ratio of 4 and a complexation constant equal to 3.3×10^{12}. It was proposed that this increase in the stoichiometric equivalents of CMPO is the result of an increase in ion−ion or ion-pair formation between rubidium and sulfate.

Our recently developed ESI-MS analysis of emulsions formed by shaking the water and DCE phases is a powerful tool to corroborate the complex stoichiometry obtained by electroanalytical chemistry at micro w|DCE interfaces.

ASSOCIATED CONTENT

Supporting Information

Thermodynamics diagram of ion transfer, extended blank w|DCE CV, and 25-μm-diameter micropipet fabrication. This material is available free of charge via the Internet at http://pubs.acs.org.

AUTHOR INFORMATION

Corresponding Author

*Tel.: +1 519 661-2111 ext 86161. Fax: +1 519 661-3022. E-mail: zfding@uwo.ca. URL: http:// http://publish.uwo.ca/~zfding/.

Notes

The authors declare no competing financial interest.

ACKNOWLEDGMENTS

We would like to thank J. Clara Wren, Jamie Noël, David W. Shoesmith, Paul J. Ragogna, Jonathan Dube, Kalen Swanick, Jing Zhang, Daniel Vaccerello, John Vanstone, Jon Aukima, Justin Smith, Doug Hairsine, Sherrie McPhee, and Marylou Hart for their helpful discussions and technical support. This work was supported by the ORF, NSERC, CFI, OIT, PREA, and The University of Western Ontario.

REFERENCES

(1) Hoffert, M. I.; Caldeira, K.; Benford, G.; Criswell, D. R.; Green, C.; Herzog, H.; Jain, A. K.; Kheshgi, H. S.; Lackner, K. S.; Lewis, J. S.; Lightfoot, H. D.; Manheimer, W.; Mankins, J. C.; Mauel, M. E.; Perkins, L. J.; Schlesinger, M. E.; Volk, T.; Wigley, T. M. L. *Science* **2002**, *298*, 981−987.

(2) Robens, E.; El Nokraschy, H.; Dąbrowski, A. *Annal. UMCS, Chem.* **2008**, *63*, 94−110.

(3) Murray, J.; King, D. *Nature* **2012**, *481*, 433−435.

(4) Nash, K. L. In *Separations for the Nuclear Fuel Cycle in the 21st Century*; Lumetta, G. J., Nash, K. L., Clark, S., B., Friese, J. I., Eds.; American Chemical Society: Washington, DC, 2006; pp 22−40.
(5) Shoesmith, D. W. *J. Nucl. Mater.* **2000**, *282*, 1−31.
(6) Bruno, J.; Ewing, R. C. *Elements (Chantilly, VA, U.S.)* **2006**, *2*, 343−349.
(7) Bonardi, M. L.; Martano, L.; Groppi, F.; Chinol, M. *Appl. Radiat. Isot.* **2009**, *67*, 1874−1877.
(8) Ciavardelli, D.; D'Anniballe, G.; Nano, G.; Martin, F.; Federici, G.; Sacchetta, P.; Di, I. C.; Urbani, A. *Rapid Commun. Mass Spectrom.* **2007**, *21*, 2343−2350.
(9) Aksenov, N. V.; Bruchertseifer, H.; Starodub, G. Y.; Vostokin, G. K.; Tereshatov, E. E.; Bozhikov, G. A.; Shishkin, S. V.; Dmitriev, S. N. *J. Radioanal. Nucl. Chem.* **2009**, *279*, 341−343.
(10) Alvarez-Diez, T. M.; deKemp, R.; Beanlands, R.; Vincent, J. *Appl. Radiat. Isot.* **1999**, *50*, 1015−1023.
(11) Yoshinaga, K.; Klein, R.; Tamaki, N. *J. Cardiol.* **2010**, *55*, 163−173.
(12) Dhar, R.; Ananthasubramaniam, K. *Cardiol. Rev.* **2011**, *19*, 255−263.
(13) Wester, D. W.; Steele, R. T.; Rinehart, D. E.; DesChane, J. R.; Carson, K. J.; Rapko, B. M.; Tenforde, T. S. *Appl. Radiat. Isot.* **2003**, *59*, 35−41.
(14) Stockmann, T. J.; Lu, Y.; Zhang, J.; Girault, H. H.; Ding, Z. *Chem.—Eur. J.* **2011**, *17*, 13206−13216.
(15) Paiva, A. P.; Malik, P. *J. Radioanal. Nucl. Chem.* **2004**, *261*, 485−496.
(16) Dai, S.; Ju, Y. H.; Barnes, C. E. *J. Chem. Soc., Dalton Trans.* **1999**, 1201−1202.
(17) Visser, A. E.; Jensen, M. P.; Laszak, I.; Nash, K. L.; Choppin, G. R.; Rogers, R. D. *Inorg. Chem.* **2003**, *42*, 2197−2199.
(18) Dietz, M. L.; Stepinski, D. C. *Talanta* **2008**, *75*, 598−603.
(19) Stepinski, D. C.; Vandegrift, G. F.; Shkrob, I. A.; Wishart, J. F.; Kerr, K.; Dietz, M. L.; Qadah, D. T. D.; Garvey, S. L. *Ind. Eng. Chem. Res.* **2010**, *49*, 5863−5868.
(20) Kakiuchi, T.; Senda, M. *J. Electroanal. Chem.* **1991**, *300*, 431−445.
(21) Homolka, D.; Holub, K.; Marecek, V. *J. Electroanal. Chem. Interfacial Electrochem.* **1982**, *138*, 29−36.
(22) Reymond, F.; Lagger, G.; Carrupt, P.-A.; Girault, H. H. *J. Electroanal. Chem.* **1998**, *451*, 59−76.
(23) Girault, H. H. J.; Schiffrin, D. J. In *Electroanalytical Chemistry*; Bard, A. J., Ed.; Marcel Dekker: New York, 1989; Vol. *15*, pp 1−141.
(24) Samec, Z.; Langmaier, J.; Kakiuchi, T. *Pure Appl. Chem.* **2009**, *81*, 1473−1488.
(25) Girault, H. In *Electroanalytical Chemistry*; Bard, A. J., Zoski, C. G., Eds.; CRC Press: 2010, p 1−104.
(26) Taylor, G.; Girault, H. H. *J. Electroanal. Chem. Interfacial Electrochem.* **1986**, *208*, 179−183.
(27) Campbell, J. A.; Girault, H. H. *J. Electroanal. Chem. Interfacial Electrochem.* **1989**, *266*, 465−469.
(28) Stockmann, T. J.; Ding, Z. *Anal. Chem.* **2011**, *83*, 7542−7549.
(29) Stockmann, T. J.; Olaya, A. J.; Méndez, M. A.; Girault, H. H.; Ding, Z. *Electroanalysis* **2011**, *23*, 2677−2686.
(30) Kakiuchi, T.; Tsujioka, N. *Electrochem. Commun.* **2003**, *5*, 253−256.
(31) Ishimatsu, R.; Shigematsu, F.; Hakuto, T.; Nishi, N.; Kakiuchi, T. *Langmuir* **2007**, *23*, 925−929.
(32) Langmaier, J.; Samec, Z. *Electrochem. Commun.* **2007**, *9*, 2633−2638.
(33) Langmaier, J.; Trojanek, A.; Samec, Z. *Electroanalysis* **2009**, *21*, 1977−1983.
(34) Stockmann, T. J.; Ding, Z. *J. Electroanal. Chem.* **2010**, *649*, 23−31.
(35) Stockmann, T. J.; Zhang, J.; Wren, J. C.; Ding, Z. *Electrochim. Acta* **2012**, *62*, 8−18.
(36) Monroe, M. http://ncrr.pnnl.gov/software/; Pacific Northwest National Laboratory, U.S. Department of Energy: Richland, WA; Accessed May 2012.
(37) Parker, A. J. *Electrochim. Acta* **1976**, *21*, 671−679.
(38) Cox, B. G.; Parker, A. J. *J. Am. Chem. Soc.* **1973**, *95*, 6879−6884.
(39) Zhurov, K.; Dickinson, E. J. F.; Compton, R. G. *J. Phys. Chem. B* **2011**, *115*, 6909−6921.
(40) Hundhammer, B.; Solomon, T. *J. Electroanal. Chem. Interfacial Electrochem.* **1983**, *157*, 19−26.
(41) Bard, A. J.; Faulkner, L. R. *Electrochemical Methods: Fundamentals and Applications*; 2nd ed.; John Wiley: New York, 2001.
(42) Shao, Y.; Osborne, M. D.; Girault, H. H. *J. Electroanal. Chem. Interfacial Electrochem.* **1991**, *318*, 101−109.
(43) Reymond, F.; Carrupt, P.-A.; Girault, H. H. *J. Electroanal. Chem.* **1998**, *449*, 49−65.
(44) Shao, Y.; Stewart, A. A.; Girault, H. H. *J. Chem. Soc., Faraday Trans.* **1991**, *87*, 2593−2597.
(45) Olaya, A. J.; Méndez, M. A.; Cortes-Salazar, F.; Girault, H. H. *J. Electroanal. Chem.* **2010**, *644*, 60−66.
(46) Leize, E.; Jaffrezic, A.; Van Dorsselaer, A. *J. Mass Spectrom.* **1996**, *31*, 537−544.
(47) Neander, S.; Behrens, U.; Olbrich, F. *J. Organomet. Chem.* **2000**, *604*, 59−67.
(48) Frenzel, C.; Somoza, F., Jr.; Blaurock, S.; Hey-Hawkins, E. *J. Chem. Soc., Dalton Trans.* **2001**, 3115−3118.
(49) Lawrance, G. A.; Robertson, M. J.; Sutrisno; von Nagy-Felsobuki, E. I. *Inorg. Chim. Acta* **2002**, *328*, 159−168.
(50) Chekhlov, A. *Russ. J. Coord. Chem.* **2007**, *33*, 482−487.
(51) Torvisco, A.; Decker, K.; Uhlig, F.; Ruhlandt-Senge, K. *Inorg. Chem.* **2009**, *48*, 11459−11465.
(52) Hill, M. S. *Annu. Rep. Prog. Chem., Sect. A: Inorg. Chem.* **2009**, *105*, 55−74.
(53) Mähler, J.; Persson, I. *Inorg. Chem.* **2011**, *51*, 425−438.
(54) Meng, Y. *Acta Crystallogr., Sect. E: Struct. Rep. Online* **2011**, *67*, m454.
(55) Fujii, T.; Aoki, K.; Yamana, H. *Solvent Extr. Ion Exch.* **2006**, *24*, 347−357.
(56) Siddall, T. H., III *J. Inorg. Nucl. Chem.* **1963**, *25*, 883−892.
(57) Holden, N. E. In *CRC Handbook of Chemistry and Physics*; Haynes, W. M., Ed.; CRC Press/Taylor: Boca Raton, FL, 2011; Vol. *91*, pp 11−82.
(58) Wang, Y.; Kakiuchi, T.; Yasui, Y.; Mirkin, M. V. *J. Am. Chem. Soc.* **2010**, *132*, 16945−16952.
(59) Mantina, M.; Valero, R.; Cramer, C. J.; Truhlar, D. G. In *CRC Handbook of Chemistry and Physics*; Haynes, W. M., Ed.; CRC Press/Taylor: Boca Raton, FL, 2012; Vol. *92*, pp 9−49.
(60) Gil-Ramírez, G.; Benet-Buchholz, J.; Escudero-Adán, E. C.; Ballester, P. *J. Am. Chem. Soc.* **2007**, *129*, 3820−3821.
(61) Ahman, A.; Luostarinen, M.; Rissanen, K.; Nissinen, M. *New J. Chem.* **2007**, *31*, 169−177.
(62) Méndez, M. A.; Su, B.; Girault, H. H. *J. Electroanal. Chem.* **2009**, *634*, 82−89.